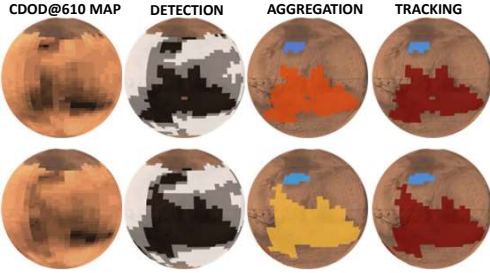


INTRODUCTION

Martian dust storms significantly impact the planet's climate and weather, influencing both atmospheric and surface conditions [1]. Orbital data help track these storms, which pose challenges for spacecraft operations and energy production [2], [3], [4] and [5]. Accurate monitoring and forecasting are crucial for future Mars exploration [6]. Previous work has utilized supervised machine learning (SML) for detecting dust storms from visible images, but this study explores the use of Unsupervised Machine Learning (UML) for detecting, aggregating, and tracking Martian dust events using infrared atmospheric data.



DATA

The study employs the column dust optical depth dataset at 610 Pa pressure level (CDOD@610) spanning from Martian Year (MY) 24 to 36 [9]. This dataset, normalized to remove topographic features, includes gridded observation maps and kriged maps from satellite retrievals. The focus is on detecting large-scale dust events with surface areas $\geq 1.6 \times 10^6 \text{ km}^2$ lasting more than two Martian days [2]. If you are interested please follow the QR code links to access the databases:

- New retrievals and maps of CDOD from MRO/CTES observations in MY24 to MY27 are available on the NASA/PDS.
- Maps from MRO/MCS v5.2 in MY28 to MY36 are available on the Mars Climate Database (MCD) webpage.

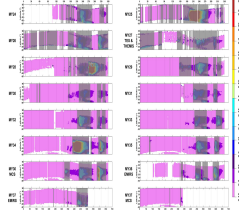


Figure 3: Detection of dust events for several Martian Years indicated by gray shaded rectangles. Zonal means of the daily irregularly gridded maps of $9.3 \mu\text{m}$ absorption column dust optical depth normalized to the reference 610 Pa pressure level for the different Martian Years, is displayed in background. Preliminary maps for MY36 from EMIRS and MY37 from both EMIRS and MCS are currently available upon request.

METHOD

Detection involves identifying spatio-temporal anomalies in CDOD maps, distinguishing foreground dust anomalies from the background dust level using segmentation. The data is partitioned using the k-means algorithm ([13]), separating it into background dust, dust core, and dust cloud categories. Aggregation is done using the Density-Based Spatial Clustering of Applications with Noise (DBSCAN) algorithm [14]. It is used for spatial clustering of the highest CDOD values (dust core), identifying individual dust instances. These instances are tracked from one Martian day (Sol) to another, forming sequences based on spatial coherence and continuity.

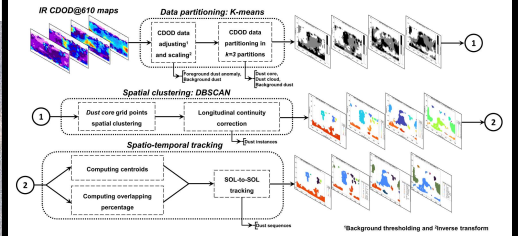


Figure 2: Flow chart of the proposed approach ST-DATMADE.



Image Credit: NASA/JPL-Caltech/MSSS

RESULTS

The ST-DATMADE approach successfully detects, aggregates, and tracks dust events across multiple Sols, demonstrating the method with data around $L_S = 228^\circ$ during MY24, around $L_S = 187^\circ$ during MY25, around $L_S = 35^\circ$ during MY35 and around $L_S = 311^\circ$ during MY36. The study produces a catalog of dust event instances, identifying their spatio-temporal distribution and statistical features such as area and intensity.

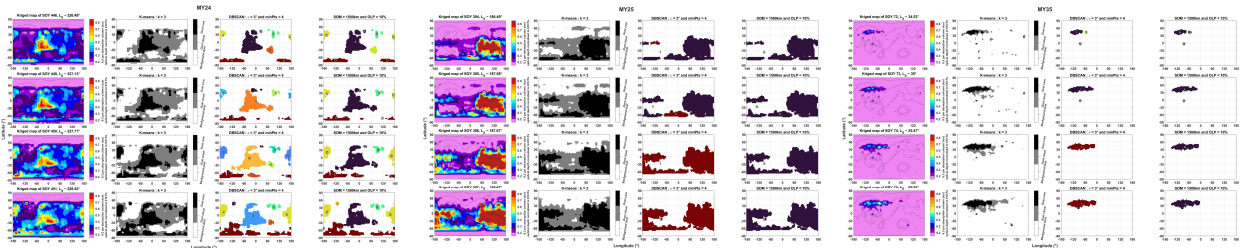


Figure 4: Martian dust event detection (second column), aggregation into instances (numbers in third column) and tracking of sequences (letters and colors in fourth column) from kriged maps (first column). Montabone et al., 2015 defined a Sol-of-Year from a Sol-based Martian calendar, where MYs have an integer number of Sols [9]. One may note that only sequences lasting more than 2 Sols are labelled with a letter. Left panel: MY24, around $L_S = 228^\circ$ between Sol-of-Year (SOY) 448 and 451. Center panel: MY25, around $L_S = 187^\circ$ between Sol-of-Year (SOY) 384 and 387. Right panel: MY35, around $L_S = 35^\circ$ between Sol-of-Year (SOY) 72 and 75.

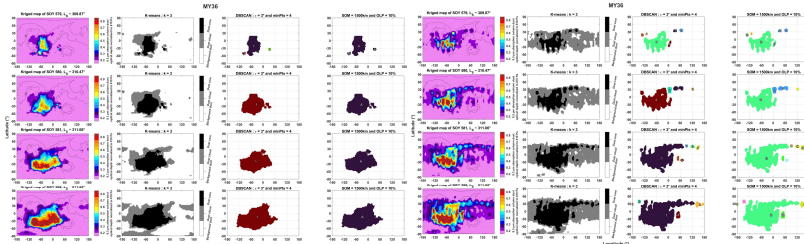


Figure 5: Martian dust event detection (second column), aggregation into instances (numbers in third column) and tracking of sequences (letters and colors in fourth column) from kriged maps (first column), during Montabone et al., 2015 defined a Sol-of-Year from a Sol-based Martian calendar, where MYs have an integer number of Sols [9]. Left panel: MY35, around $L_S = 311^\circ$ between Sol-of-Year (SOY) 579 and 582 maps (using EMIRS instrument data). Right panel: MY36, around $L_S = 311^\circ$ between Sol-of-Year (SOY) 579 and 582 (using MCS instrument data).

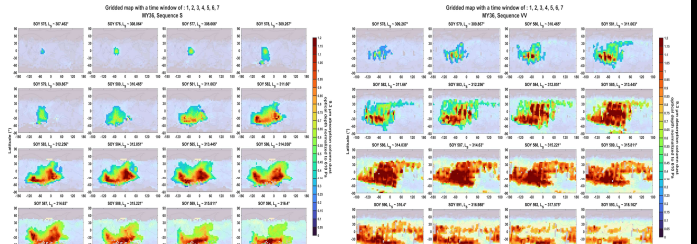


Figure 6: Sol-by-sol identification and tracking of the evolution of a dust sequence ("storm"). The rest of the daily gridded maps is visible in the transparent background. Left panel: MY36 between $L_S = 307^\circ$ and $L_S = 316^\circ$ from daily EMIRS-based CDOD maps normalized to 610 Pa. Right panel: MY36 between $L_S = 309^\circ$ and $L_S = 318^\circ$ from daily MCS-based CDOD maps normalized to 610 Pa.

CONCLUSIONS

The automatic, Unsupervised Machine Learning-based approach effectively detects and tracks Martian dust events, providing a comprehensive analysis of their spatio-temporal characteristics. This method offers a more objective and detailed understanding of dust storm behavior compared to previous human-based visual inspections.

PERSPECTIVES

The developed catalog will facilitate in-depth studies of large-scale dust events, including their origins, trajectories, and seasonal behavior. The methodology reduces subjectivity and improves the accuracy of dust storm detection, supporting future Mars exploration efforts and paving the way towards future dust storm forecasting.

ACKNOWLEDGMENTS

The authors would like to acknowledge the use of the publicly available dataset on the LMD webpage and the NASA PDS webpage (see QR code links). L. Montabone acknowledges contract with CNRS.

REFERENCES

[1] L. Montabone and F. Forget, 2018, <http://hdl.handle.net/2346/74226>
 [2] B. A. Cantor et al., 2001, doi: 10.1029/2000JE001310.
 [3] H. Wang and M. I. Richardson, 2015, doi: 10.1016/j.icas.2013.10.033.
 [4] M. Battalio and H. Wang, 2021, doi: 10.1016/j.icas.2020.114059.
 [5] C. Gebhardt et al., 2022, https://www.mars.lmd.jussieu.fr/pairs2022/abstracts/poster_Gebhardt_Claus.pdf
 [6] L. Montabone, 2022, https://www.mars.lmd.jussieu.fr/pairs2022/abstracts/orig_Montabone_Luca.pdf
 [7] R. Alshewhi and C. Gebhardt, 2022, doi: 10.1186/s40645-021-00464-1.
 [8] K. Oghara and R. Gichu, 2022, doi: 10.1016/j.cageo.2022.105043.
 [9] L. Montabone et al., 2015, doi: 10.1016/j.icas.2014.12.034.
 [10] L. Montabone et al., 2020, doi: 10.1029/2019JE006111.
 [11] F. Forget and L. Montabone, 2017, <http://hdl.handle.net/2346/72982>
 [12] B. G. Tabachnick and L. S. Fidell, Using Multivariate Statistics, Pearson Education, 2013.
 [13] S. Lloyd, 1982, doi: 10.1109/TIT.1982.1056489.
 [14] M. Ester et al., 1996, <https://www2.cs.uh.edu/~ceick/7363/Papers/dbscan.pdf>
 [15] D. M. Kass et al., 2016, doi: 10.1002/2016GL068978.